PCCP

PAPER

View Article Online
View Journal

Cite this: DOI: 10.1039/d5cp02381e

Reactivity of polonium towards quartz surfaces

Katharina Hermainski, *[a] Alexander Yakushev, [b] Dominik Dietzel, [ab] Christoph Emanuel Düllmann, [abc] Jochen Ballof, [b] Pavol Mošat', [b] Felix Sprunk, [ab] Pavel Bartl, [d] Jan John, [d] Jörg Krier,[b] Mojmír Němec, [d] Jon Petter Omtvedt [e] and Jan Štursa [f]

Beyond the (quasi)stable and abundant elements lead and bismuth, all elements are radioactive, with polonium being the first of a series of radioelements up to primordial uranium. Interest in understanding its chemical behavior is increasing, not least due to its co-production in accelerator-driven systems and high radiotoxicity. Polonium is also the lighter homologue of the superheavy element livermorium, which has not been studied chemically to date. Polonium therefore acts as a benchmark to verify the structure of the periodic table at the heavy-element frontier. Here, we report on gas–solid thermochromatography studies of polonium in the atom-at-a-time regime under helium and hydrogen gas atmospheres. Quartz surfaces with different degrees of hydroxylation were used as a stationary phase. On quartz glass with low OH-concentrations, a volatile species interacting with an adsorption enthalpy of -85^{+3}_{-2} kJ mol^{-1} was found and assigned to elemental polonium. On more highly hydroxylated quartz glass, an additional deposition zone due to a species with an adsorption enthalpy of -139^{+6}_{-5} kJ mol^{-1} was observed and attributed to a polonium species formed by chemical reactions with the surface. Under our experimental conditions, chemical reactions of polonium in the solid phase dominate over reactions in the gas phase. Thus, the nature of the surface should be considered as an important parameter in future gas chromatography studies.

Received 23rd June 2025,
Accepted 29th August 2025

DOI: 10.1039/d5cp02381e

rsc.li/pccp

Introduction

The discovery of polonium was the first time that non-visible quantities of an element were detected solely by its characteristic radiation.[1] Besides the quasi-stable bismuth, polonium is the first radioelement of the periodic table which occurs naturally through the α decay of thorium or uranium.[2] Studies of the element have, due to its high radiotoxicity, often been limited to characterizing it in the environment and to studying its uptake in living organisms.[2,3] The development of so-called accelerator-driven systems,[4] which aim for the transmutation of long-lived, radiotoxic actinides in spent nuclear fuel, has moved polonium further into focus. In these systems, polonium is produced by the interaction of protons or neutrons with bismuth, which is used in the form of lead-bismuth eutectic as a reactor coolant or a spallation target. Thus, the gas phase chemistry of polonium is of particular interest for the safe operation and the safe handling of target materials in these systems.[5–7]

In addition, the chemistry of polonium is now also moving further into focus from the perspective of superheavy element studies. Since the first investigations of rutherfordium in the 1960s, chemical investigations of transactinides have progressed to moscovium (atomic number Z = 115).[8–12] The study of these superheavy elements (SHE) contributed to a better understanding of the influence of relativistic effects on chemistry.[13] Due to the complex production of SHE in nuclear heavy ion fusion reactions and their short half-lives, the chemical study of SHE requires highly efficient techniques. Often, automated experiments are performed that enable the study of single atoms.[10,14,15] A first step towards the chemical investigation of the still experimentally uncharacterized and very short-lived ($t_{1/2}(^{293}\mathrm{Lv}) = 95^{+63}_{-27}$ ms)[16] element livermorium (Z = 116) is the analysis of its lighter homologue polonium (Z = 84).

Macroscopic amounts of polonium crystallize at room temperature in an exceptionally rare, simple cubic structure (α-Po). At higher temperatures (above 36 °C), polonium crystallizes rhombohedrally (β-Po). The melting point of the element is 254 °C, and its boiling point is 962 °C.[17] Polonium occurs in the

[a] Johannes Gutenberg University Mainz, 55099 Mainz, Germany. E-mail: kahermai@uni-mainz.de
[b] GSI Helmholtzzentrum für Schwerionenforschung GmbH, 64291 Darmstadt, Germany
[c] Helmholtz Institute Mainz, 55099 Mainz, Germany
[d] Czech Technical University in Prague, 115 19 Prague, Czech Republic
[e] University of Oslo, 0315 Oslo, Norway
[f] Nuclear Physics Institute CAS, 250 68 Husinec-Řež, Czech Republic

oxidation states −2 (as polonide), 0, +2, +4 and +6, with the +4 oxidation state being the most stable.[1,17] The high specific activity of any macroscopic polonium sample poses not only a hazard when handling polonium but also leads to self-heating of specimens under investigation, affecting temperature-dependent measurements. Due to the positive temperature resistance coefficient, and the decreasing electronegativity and first ionization energy from tellurium to polonium, the element can be classified as a metal.[18] Polonium has mainly been studied in the liquid phase, whereas relatively few studies in the gas phase have been reported. It is known from classical chemical studies of polonium that the metal can be slowly oxidized at room temperature in air to form the dioxide. The reaction is most rapid at 250 °C.[19,20] In addition to the polonium dioxide, both the monoxide and the trioxide have been isolated; however both these oxides could not previously be obtained directly from the elements.[18,21] Also, polonium hydride cannot be produced directly from the elements.[20] Instead, it could previously only be obtained in trace amounts by reduction with nascent hydrogen under light and oxygen exclusion.[1,17,20] The stability of the hydrides decreases within the group of chalcogens with Z due to the increasing atom size and thus increasing bond length. Polonium hydride is known to be volatile.[20,22]

To investigate the gas phase chemistry of (short-lived) superheavy elements and their homologues, gas chromatography (GC) experiments have proven to be particularly useful.[10,11] In thermochromatography,[10] a negative temperature gradient is applied along the column. In a simple picture, the element to be analysed is transported through the column by the gas flow, interacts with the column and is adsorbed at a certain deposition temperature determined by its adsorption enthalpy.[23] Materials such as gold or SiO_2 (quartz) are chosen for the solid phase, as they are mostly unreactive towards the mobile phase and reactive towards the analysed elements. The strength of an atom's interaction with metal surfaces, such as gold, can indicate whether the element should be classified as a metal. This is because metals are capable of forming strong metallic bonds with the surface, resulting in a higher measured deposition temperature. This technique has been successfully implemented to study the superheavy elements copernicium (Z = 112) to moscovium.[10–12] Through the addition of reactive gases such as oxygen or hydrogen, the formation and volatility of different chemical compounds can be investigated. Gas chromatographic analysis of the long-lived radioisotopes of homologues of SHE is usually possible with simple open quartz glass tubes, possibly lined with metal foils.[24] For the chemical investigation of SHE, the use of the narrow channel formed by arrays of silicon detectors as a chromatography column became established.[10] To allow a better comparability of homologue studies with the chemistry of their corresponding SHE, homologue experiments are often also performed at the atom-at-a-time scale. In such experiments, the homologues are mostly produced in nuclear reactions at accelerator facilities in single-atom quantities.[11]

Since a majority of the 6p-elements exhibit a metallic behavior,[25–28] the resulting high affinity to metal surfaces renders the separation of the elements on gold at room temperature challenging.[5,24,29] As an alternative, SiO_2-coated detectors were successfully used in past experiments to chemically analyse the superheavy elements nihonium (Z = 113) and moscovium.[12] Due to the unpaired $7p_{3/2}$-electrons, a similar reactivity to that of nihonium and moscovium is expected for livermorium.[30] Thus, studying the interaction of its homologue polonium with quartz is of interest.

The primary functional groups on the surface of quartz are siloxane (Si–O–Si bridges) and silanol (Si–OH) groups.[31–33] The reactivity of the quartz surface is primarily determined by the density of silanol groups on the surface.[34] The initial silanol concentration varies for different quartz glass production methods. If a hydrogen–oxygen flame is used to melt the quartz granulate, the hydroxyl content on the surface is higher, whereas electro-melting the quartz in a vacuum results in a comparatively low hydroxyl concentration.[35,36] The concentration of silanol groups on the surface can be reduced by annealing the quartz glass under an inert gas atmosphere at high temperatures (1000 °C).[34–36] Heating the quartz glass in an atmosphere with sufficient water or hydrogen concentration increases the amount of silanol groups and therefore the reactivity of the surface.[37–40] Knowledge of the surface structure is crucial for gas chromatography experiments, as the interaction strength can vary significantly depending on the local site reactivity.[41,42]

In GC experiments with SHE and homologues, the deposition profile of the element of interest is measured. The adsorption enthalpy $-\Delta H_{ads}$, a measure of the volatility of a species, can be extracted from the deposition temperature using the Monte Carlo method by Zvára based on reversible adsorption.[43] In this method, the migration of an atom or a molecule downstream the column is simulated by a series of displacements and adsorption–desorption cycles. By simulating multiple thousand atoms or molecules, a deposition pattern is obtained. The only free parameter in the simulation is the adsorption enthalpy. The adsorption enthalpy is varied, until the best match of the experimental deposition profile with the simulated deposition profile is obtained. In contrast to the deposition temperature, the enthalpy of adsorption is independent of effects due to variations in experimental parameters such as the gas flow rate. It is thus solely defined by the adsorption interaction with the surface.

The Monte Carlo method by Zvára has proven to be a highly valuable tool due to its advantages such as the easy adaptability of the simulation to experimental conditions.[42,44,45] However, the simulation is based on several assumptions and approximations that do not always hold true. One example is the assumption of simple reversible adsorption of unchanged molecules which is only correct if no chemical reactions are involved in the interaction of the analysed species with the surface. However, especially for inhomogeneous surfaces with sites of different reactivities such as on quartz, the possibility that the desorbed species is different to the adsorbed one cannot be neglected.[33]

Here, we investigate the chemistry of polonium by thermochromatography on quartz glass under helium and hydrogen

atmospheres. In previous work, the adsorption enthalpy of polonium on quartz was found to be around 85 kJ mol^{-1} by Eichler,[46] Vogt *et al.*[47] and Gärtner.[48] However, a more recent publication by Maugeri *et al.* suggests a significantly higher adsorption enthalpy of 120–140 kJ mol^{-1}.[49] While previous work has mostly focused on the influence of different reactive gases on the deposition profile of polonium,[49] we also take the influence of the quartz surface into account. In this paper, we show that a reaction of polonium with the quartz surface depends on the degree of hydroxylation, which itself is a function of the surface temperature and the composition of the carrier gas.

Experimental

Thermochromatography experiments involving radioactive nuclei can only be carried out in licensed laboratories under appropriate radiation protection regulations. Here, the experiments were carried out at the U-120M cyclotron facility at the Nuclear Physics Institute of the Czech Academy of Sciences in Řež (Czech Republic) using the MARGE (Modular Robotic Gas-Jet Target System) beamline and a recoil transfer chamber.[50] Single-atom quantities of ^{204}Po and ^{205}Po were produced in the nuclear reaction ^{206}Pb(^{3}He, 4–5n)^{204,205}Po through bombardment of an enriched ^{206}Pb target with a 48-MeV ^{3}He beam. The target material was deposited on a titanium backing (2.3 μm or 5 μm). Recoiling nuclei were collected in 2.5 μm-thick titanium or 75 μm-thick carbon catcher foils mounted about 1 mm behind the target. The target chamber was kept at 1 bar in helium. This nuclear reaction allows higher beam energies compared to α-induced reactions and allows for comparatively short irradiation times due to the shorter half-life of the produced polonium isotopes. We estimate that a few million polonium atoms are produced by this reaction per hour, not taking the radioactive decay of the atoms into account. The experimental setup used for thermochromatography is illustrated in Fig. 1. The abbreviations for experiments used in the following discussions indicate the gas and the type of quartz (surface) used. Here, He describes a gas atmosphere of 100% helium and H2 an atmosphere of 10% hydrogen and 90% helium. The different types of quartz Q1, Q2 and Q3 are indicated as an index. Technical details on the devices and materials used in this work can be found in the SI.

For thermochromatography experiments, quartz glass tubes (length 82 or 90 cm) with different densities of silanol groups and thus different surface reactivities were employed. The tubes, arranged by increasing reactivity of the inner surface, include (i) tubes produced recently by electromelting of a quartz granulate in a vacuum (Q1), (ii) older quartz glass that was heat-treated at 1000 °C for multiple hours under an inert gas atmosphere by us prior to the experiment (Q2), and (iii) older, thermally untreated quartz glass which was stored under standard laboratory atmosphere (no water-free conditions, Q3).

The temperature gradient applied along the column was established using three tube furnaces at the beginning and copper coils with flowing cooling water at the end of the column. The temperature of the tube furnaces could be regulated individually by applying different voltages to the ovens. The catcher foil containing the produced polonium atoms was placed inside the quartz column in the middle of the first furnace, corresponding to the hottest zone (400 to 1030 °C, see Table S1 of the SI) of the column. In experiments $\mathbf{He_{Q2}}$ and $\mathbf{H2_{Q3}}$ (column length: 82 cm), a greater distance was chosen between the first furnace used for heating the catcher foil and the second furnace. In this case, the temperature gradient relevant to chromatography starts at the second furnace; in all other experiments, it starts in the first furnace for baking-out the catcher foil. The efficiencies to evaporate polonium from the catcher foil, as well as the irradiation time, the time that elapsed between the end of irradiation and the beginning of the experiment, and the extraction efficiencies into the

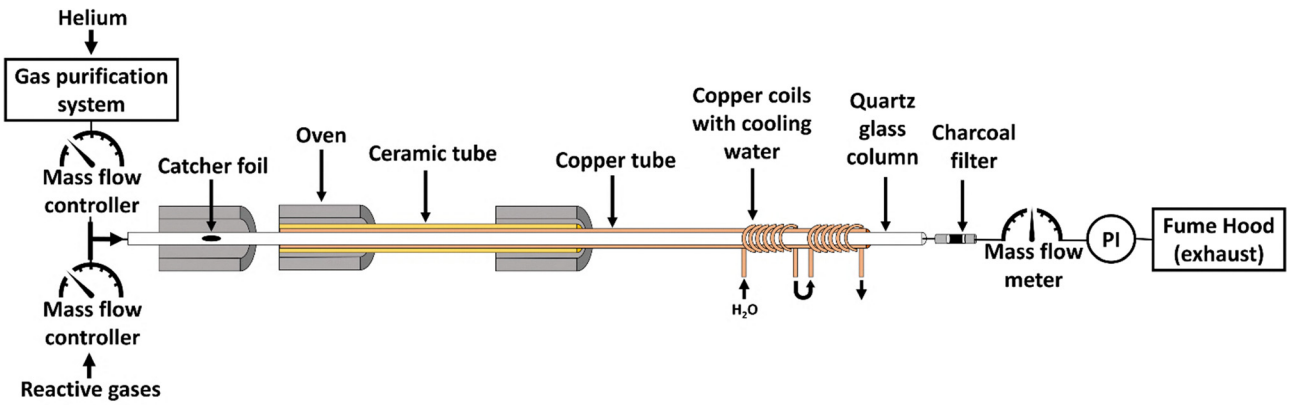

Fig. 1 Schematic of the thermochromatography setup used in this work. Helium flushes through the gas purification system and into the quartz column. Reactive gases are mixed with helium before the column. The gas flow rate of both gases is regulated using mass flow controllers. The column is heated by three furnaces, the first of which is used to evaporate the polonium atoms from the catcher foil. A copper and a ceramic tube as well as a water-cooling system help to establish the temperature gradient. An activated charcoal filter traps the activity passing through the column. After the filter, the gas flow and the pressure are monitored with a mass flow meter and a pressure indicator (PI). The gas passed through the experimental setup is exhausted into a fume hood.

chromatography column in experiments $\mathbf{He_{Q2}}$ and $\mathbf{H2_{Q3}}$ are given in Table S1 of the SI. Before the irradiated catcher foil was inserted in the experiment, its γ spectrum was measured to identify the nuclide inventory.

To smoothen the temperature gradient, the quartz tube was partially inserted into a 78.5 cm-long copper and a 42 cm-long ceramic tube of which the outer diameter matched the inner diameter of the tube furnaces, as shown in Fig. 1. The helium carrier gas was purified by using several cartridges (see the SI) to reduce water and oxygen impurities before it passed through the experimental setup. Hydrogen pre-mixed with helium (60% helium/40% hydrogen) could be added to the carrier gas *via* a ball valve. The gas was led to the experiment using polytetrafluoroethylene (PTFE) or stainless-steel capillaries. The helium and the helium/hydrogen mixture flow rates (100 sccm min^{-1} in experiment $\mathbf{He_{Q1}}$ **II** and 50 sccm min^{-1} in all other experiments) were controlled with two mass flow controllers. To monitor possible gas leaks in the experiment, a mass flow meter was employed to measure the gas flow rate after the column. In addition to the gas flow rate, the pressure behind the column was measured using a pressure indicator. Radioisotopes passing through the column were collected in an activated charcoal filter inside a Teflon tube with the same dimensions as the quartz tube. All connections were made from stainless steel Swagelok compression fittings or push-in fittings made from polybutylene terephthalate.

For each experiment, the chromatography column with catcher foil was heated for 1–2 h with the gas flow running. During this time, polonium atoms were thermally released from the catcher foil and transported with the gas flow into the chromatography column where they would form a distinct deposition pattern. To ensure a constant temperature gradient and gas flow during the experiment, the temperature of the ovens and the gas flow rate were continuously monitored.

After the experiment, the gas flow was stopped, and the column was removed from the furnaces through the cold end and sealed with septum caps. After cooling down to room temperature, the column was cut into (2.0 ± 0.2) cm or (4.0 ± 0.2) cm pieces from the end back to the position of the catcher foil. Each piece was sealed in a plastic sample container. Subsequently, γ spectra of the samples of the column containing the polonium activity, the activated charcoal filter, and the catcher foil were measured with a HPGe-detector (see the SI for technical details). A 3D-printed sample holder was used on the detector to ensure consistent measurement geometry. The distance between the samples and the detector was kept at about 1 cm.

The temperature gradient was measured after each experiment, in 2-cm or 4-cm steps depending on the steepness of the gradient, using a 100 cm-long type-K thermocouple attached to a read-out unit. The temperature error was estimated from the uncertainty of the read-out unit (0.05%) and the thermocouple (±2 °C) as specified by the manufactures and from the uncertainty of the placement of the thermocouple (±5 mm). As the temperature gradient became steeper towards higher temperatures, the uncertainty of the placement of the thermocouple causes a larger temperature error at higher temperatures.

To obtain the thermochromatograms, the γ lines of ^{204}Po (884 keV, I_γ = 29.9%; 1016 keV, I_γ = 24.1%) and ^{205}Po (872 keV, I_γ = 37.0%; 1001 keV, I_γ = 28.8%) were integrated in all γ spectra of the individual column segments. They were then baseline-, dead time- and decay-corrected, and normalized to the measurement time. To obtain the relative deposition yields per 2 cm or 4 cm, the obtained net peak areas were normalized to the total activity (sum of all corrected integrals) in the column. The uncertainty in the length of the column segments resulting from the cutting of the chromatography column was added to the error of the net peak area. The deposition patterns obtained from the evaluation of the different γ lines of the same radioisotope were compared to each other to ensure that the evaluated deposition was not influenced by any other radioisotopes. In the thermochromatograms shown in this work, the deposition pattern evaluated from the strongest γ line of the longer-lived and more abundantly produced ^{204}Po is displayed, as this γ line proved to be undisturbed. In the experiment $\mathbf{He_{Q1}}$ **II**, the deposition between centimetres 42 and 50 was only measured in 4-cm steps. To obtain the deposition per 2 cm, it was assumed that the activity is equally distributed over the 4 cm.

The adsorption enthalpy was estimated by comparing the experimental results with distributions obtained from Monte Carlo simulations (MCS). Here, the original model based on reversible adsorption by Zvára was employed.[43] The most probable adsorption enthalpy value was obtained from the simulated distribution with the best fit to the experimental results. For the very broad deposition pattern in the experiment $\mathbf{He_{Q3}}$, the maximum of the simulated deposition peak was aligned with the maximum of the experimental deposition peak.

An important parameter in the Monte Carlo simulation is the lifetime of the atoms in the column. For online measurements, this time can be calculated from the half-life of the nuclide. In offline measurements as carried out here however, the ''lifetime'' (in the following replaced by the more appropriate term ''sojourn time'') is not determined by the half-life, but by the experiment time and the time at which the atoms are released from the catcher foil.[51] Based on the different implantation depths and the distribution of the diffusion velocities of the polonium atoms in the catcher foil, the individual polonium atoms are most probably not released from the catcher foil at the same time. Thus, a distribution of sojourn times results. Based on separate experiments studying the release of polonium from the catcher foil, it was assumed that all atoms leave the foil within a few minutes (between 5 and 10 min, depending on the temperature) after the start of the experiment. To take into account atoms which leave the foil directly at the beginning of the experiment or later during the experiment, the adsorption enthalpy was also determined for the upper and lower limits of the sojourn time. The deviation of this adsorption enthalpy from the enthalpy obtained with the most probable sojourn time was added to the error of the adsorption enthalpy.

In addition to the distribution of sojourn times of atoms in the column, fluctuations and errors of experimental parameters such as the gas flow rate or the temperature were taken into account in the error analysis of the adsorption enthalpy.

Results and discussion

In all the described experiments with different surface properties and gas compositions, thermochromatograms of polonium were obtained. In all experiments, no polonium was measured in the charcoal filter above the detection limit. Table 1 summarizes the most important experimental parameters and results for all conducted thermochromatography experiments in this work and assigns the measured depositions to the most probable species. The reasoning for these assignments is discussed in the following. In experiments $\mathbf{He_{Q1}}$ and $\mathbf{He_{Q2}}$, the deposition of polonium under low reactive conditions was examined. Fig. 2 shows the deposition of polonium on quartz glass Q1 ($\mathbf{He_{Q1}}$, left) and Q2 ($\mathbf{He_{Q2}}$, right) in helium. On both quartz surfaces, a single deposition peak was found at T_{dep} = (82 ± 5) °C and T_{dep} = (77 ± 7) °C, respectively. Obviously, only one species was present in the column during each experiment. From the deposition temperature in the column, the adsorption enthalpy of polonium on the quartz surfaces was extracted using the Monte Carlo method by Zvára. This led to the adsorption enthalpy values of $-\Delta H_{ads}(Po) = 85^{+3}_{-2}$ kJ mol^{-1} for experiment $\mathbf{He_{Q1}}$ and $-\Delta H_{ads}(Po)$ = (86 ± 5) kJ mol^{-1} for experiment $\mathbf{He_{Q2}}$, respectively.

For determining the adsorption enthalpy of the deposition in the experiment $\mathbf{He_{Q2}}$, two different sojourn times were adopted as input parameters for the simulation to assess the impact on the adsorption enthalpy. In the simulation which resulted in the distribution shown in blue, it was assumed that all atoms were released from the foil five minutes after the start of the experiment. In the simulation which resulted in the green distribution, it was assumed that atoms are continuously released from the catcher foil during the experiment. As can be seen in Fig. 2 (green simulation), this leads to significantly broader peaks and an adsorption enthalpy that is slightly (2 kJ mol^{-1}) less negative. In reality, the distribution of sojourn times in the column lies between these two extremes, but probably closer to the first simulation approach, which was therefore adopted for evaluating other experiments. However, as described in the Experimental section, this approach cannot correctly represent the peak form, as it does not cover the complete distribution of sojourn times.

Due to the purification of the inert carrier gas, we assume that reactive impurities were not present in sufficient concentrations to react with the polonium during the experiment. The quartz glass materials used in both experiments are expected to have a low concentration of silanol groups on the surface due to their production method (Q1, experiment $\mathbf{He_{Q1}}$) or the pretreatment of the quartz at 1000 °C under an inert gas atmosphere (Q2, experiment $\mathbf{He_{Q2}}$). Therefore, the quartz glass materials are classified as less reactive and reactions of polonium with the quartz surface are considered less likely. This would indicate a deposition of elemental polonium on the less-reactive quartz surfaces in experiments $\mathbf{He_{Q1}}$ and $\mathbf{He_{Q2}}$. However, oxygen impurities can easily adsorb on or react with the hot titanium catcher foil thus forming titanium oxide. Thus, a reaction between polonium and oxygen atoms present on or in the catcher foil cannot be excluded. For this reason, the experiment $\mathbf{He_{Q1}\ II}$ was carried out in helium with quartz Q1, but with a carbon catcher foil. A significantly lower oxygen concentration on the catcher foil in the gas phase can be assumed due to the formation of volatile carbon dioxide in the potential reaction between impurities and the carbon catcher foil. To further reduce the probability of a reaction with impurities, the temperature at the beginning of the temperature gradient was reduced significantly.

Fig. 3 shows the deposition of polonium evaporated from the carbon catcher foil on quartz Q1 in helium. In the experiment $\mathbf{He_{Q1}\ II}$, only one deposition peak at T_{dep} = (73 ± 5) °C can be detected in the chromatography column. The adsorption enthalpy extracted from the deposition temperature using the Monte Carlo simulation was found to be $-\Delta H_{ads}(Po) = 86^{+3}_{-4}$ kJ mol^{-1}. The determined adsorption enthalpy is thus in agreement with the adsorption enthalpies found in experiments $\mathbf{He_{Q1}}$ and $\mathbf{He_{Q2}}$. Since in this experiment not only reactions with the gas phase and with the quartz glass, but also with oxygen residues in/on the catcher foil seem unlikely, the deposition peaks in experiments $\mathbf{He_{Q1}}$, $\mathbf{He_{Q2}}$ and $\mathbf{He_{Q1}\ II}$ are assigned to elemental polonium. This value of $-\Delta H_{ads}$ and the assignment to elemental polonium agree well with the results of studies by Eichler (average 85.2 ± 8.9 kJ mol^{-1} in

Table 1 Summary of adsorption enthalpies $-\Delta H_{ads}$ determined with the Monte Carlo simulation from the deposition temperatures T_{dep} in all experiments, as well as the most important experimental parameters and the species to which the deposition is assigned

Experiment	Reactive gas	Quartz type	T_{dep}/°C	$-\Delta H_{ads}$/kJ mol^{-1}	Assigned species[a]
$\mathbf{He_{Q1}}$	—	Q1	82 ± 5	85^{+3}_{-2}	Po
$\mathbf{He_{Q2}}$	—	Q2	77 ± 7	86 ± 5	Po
$\mathbf{He_{Q1}\ II}$	—	Q1	73 ± 5	86^{+4}_{-3}	Po
$\mathbf{He_{Q3}}$	—	Q3	277 ± 5	139^{+6}_{-5}	$Po^{chem.}$
			67 ± 5	85^{+5}_{-3}	Po
$\mathbf{H2_{Q3}}$	Hydrogen	Q3	320 ± 10	149^{+4}_{-6}	$Po^{chem.}$
			70 ± 7	84^{+4}_{-5}	Po

[a] $Po^{chem.}$ indicates species formed *via* the reaction with the surface.

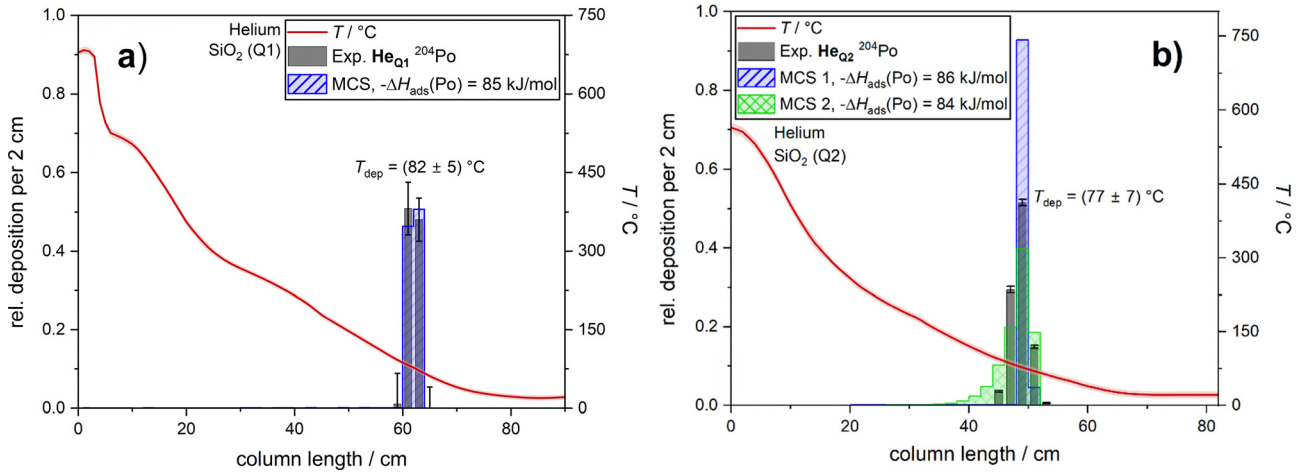

Fig. 2 Thermochromatograms of ^{204}Po in helium on quartz glass Q1 (panel (a), experiment **He$_{Q1}$**) and on quartz glass Q2 (panel (b), experiment **He$_{Q2}$**). The experimental deposition is shown in grey, the simulated deposition using the Monte Carlo simulation (MCS) is shown in blue and the temperature gradient is shown in red. Experiment **He$_{Q2}$** shows another simulation approach in green, in which different sojourn times of the atoms in the column were selected as input values (for more information, see the main text). Here, $-\Delta H_{ads}$ is the adsorption enthalpy and T_{dep} is the deposition temperature at the peak maximum.

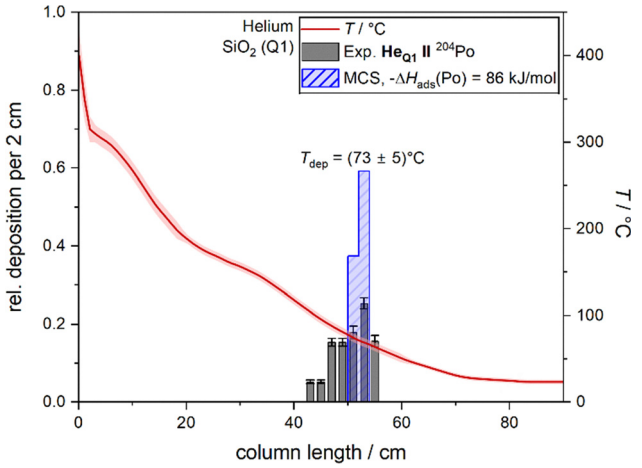

Fig. 3 Thermochromatogram of ^{204}Po evaporated from a carbon catcher foil in helium on quartz glass Q1. The experimental depositions are shown in grey, the simulated deposition using the Monte Carlo simulation (MCS) is shown in blue and the temperature gradient is shown in red. Here, $-\Delta H_{ads}$ is the adsorption enthalpy and T_{dep} is the deposition temperature at the peak maximum.

hydrogen),[46] Vogt *et al.* (85 kJ mol^{-1} in helium),[47] and Gärtner (85 ± 3 kJ mol^{-1} in He/N$_2$ and 88 ± 3 kJ mol^{-1} in Ar/H$_2$).[48] It is known that the lighter chalcogenides form molecules of the form S$_n$, Se$_n$ and Te$_n$.[17] Also, polonium can form the dimer Po$_2$.[20] Due to the single-atom concentrations in our experiments, the formation of this molecule is however excluded, as the chances of two polonium atoms meeting are very low. Thus, a direct comparison of the obtained adsorption enthalpy with the volatility of macroscopic samples of the lighter homologues is not possible. To our knowledge, only the adsorption enthalpy values of single-atom quantities of tellurium on quartz have been reported as (163 ± 10) kJ mol^{-1} and (171 ± 10) kJ mol^{-1} in two separate experiments.[52] These values point to a lower volatility of tellurium on quartz compared to polonium. The obtained deposition peak in experiment **He$_{Q1}$ II** is much broader than in the previously discussed experiments. This might point to different volatilization rates of polonium from the carbon catcher foil compared to the titanium catcher foils used in the remaining experiments.

In the experiment **He$_{Q3}$**, the deposition of polonium on untreated quartz glass Q3 in helium was evaluated. The resulting thermochromatogram is shown in Fig. 4. Two deposition

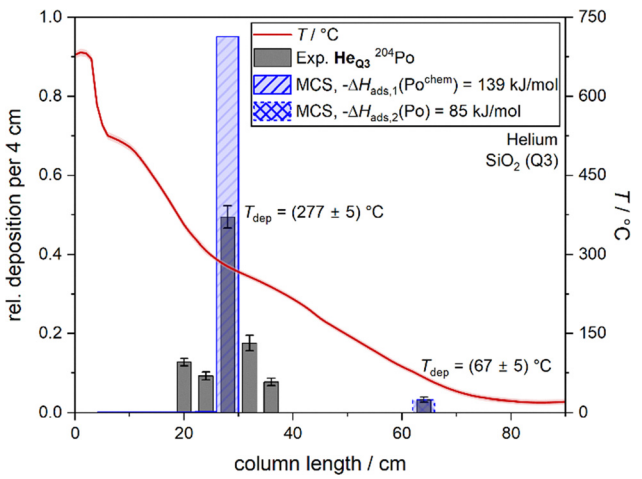

Fig. 4 Thermochromatogram of ^{204}Po in helium on quartz glass Q3. The experimental depositions are shown in grey, the simulated deposition using the Monte Carlo simulation (MCS) is shown in blue and the temperature gradient is shown in red. The relative area of the simulated deposition was scaled to the relative area of the experimental peaks. Here, $-\Delta H_{ads}$ is the adsorption enthalpy and T_{dep} is the deposition temperature at the peak maximum.

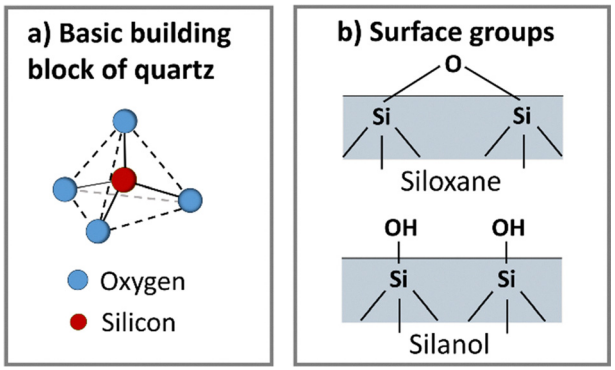

Fig. 5 Basic building block of quartz (panel (a)) and functional groups on the quartz surface (panel (b)).

peaks were observed in the column: the main deposition peak at (277 ± 5) °C comprising (97 ± 8)% of the activity, and a minor one at (67 ± 5) °C. An adsorption enthalpy of $-\Delta H_{ads}(Po^{chem}) = 139^{+6}_{-5}$ kJ mol^{-1} was obtained for the species deposited at the higher temperature using the Monte Carlo method. For the minor peak, the adsorption enthalpy of $-\Delta H_{ads}(Po) = 85^{+5}_{-3}$ kJ mol^{-1} was found. The latter is identical to the values obtained in experiments **He$_{Q1}$**, **He$_{Q2}$** and **He$_{Q1}$ II** within the range of the uncertainty. The observed difference in the deposition temperature can be attributed to the different binning of data (deposition per 2 cm *vs.* deposition per 4 cm). The adsorption enthalpy assigned to the species deposited at (277 ± 5) °C agrees with similar thermochromatography measurements of polonium on quartz in helium and hydrogen published by Maugeri *et al.*[49] The only experimental parameter changed in experiment **He$_{Q3}$** in comparison to experiments **He$_{Q1}$**, **He$_{Q2}$** and **He$_{Q1}$ II** is the quartz surface. Since no reactive gases were added to the mobile phase, a reaction of polonium with the gas phase is unlikely. Otherwise, such a reaction would be expected to have also occurred in the previously discussed experiments. If the same interaction of polonium and the surface would occur as in experiments **He$_{Q1}$**, **He$_{Q2}$** and **He$_{Q1}$ II**, only one deposition peak, corresponding to the adsorption enthalpy of about 85 kJ mol^{-1} would be expected. An increased concentration of silanol groups and thus a more reactive surface than in experiments **He$_{Q1}$**, **He$_{Q2}$** and **He$_{Q1}$ II** can be assumed in experiment **He$_{Q3}$**, since quartz Q3 was not annealed under an inert gas atmosphere. Fig. 5 shows the chemical composition of quartz (panel (a)) and the main surface groups (siloxane and silanol, panel (b)) schematically. As already shown for other oxide materials (*e.g.* Al_2O_3), the presence of hydroxide groups leads to significant changes in the properties (such as reactivity, structure or polarity) of the surface.[53,54] It is therefore very likely that the concentration of silanol groups on the surface also plays a decisive role for the deposition of polonium. In addition, the main deposition peak in the experiment **He$_{Q3}$** occurred at a significantly higher temperature than in experiments **He$_{Q1}$**, **He$_{Q2}$** and **He$_{Q1}$ II**. Considering the aspects discussed above, we attribute the deposition to a chemical reaction of polonium with the surface. The main deposition peak is also significantly broader than both the pattern obtained from the Monte Carlo simulation and the peaks observed in the previous experiments. This broadened peak cannot be explained by the distribution of the sojourn times of the atoms in the column alone and is therefore another sign that the observed adsorption process deviates from that of the model of (reversible) mobile adsorption. It is not trivial to infer exactly which reactions took place on the surface. Hydroxyl groups on the surface of alumina have proven to be a mediator for a strong interaction between a metal and the aluminium oxide surface.[55] Redox reactions on the surface of α-Al_2O_3 have already been demonstrated at room temperature for the deposition of elemental cobalt, resulting in Co^{2+} in between two O^{2-}-ions and the release of H_2.[56] It was deemed likely by the authors of that study that such a reaction is also possible for other elements and surfaces. Thus, the assumption that the polonium is oxidized and bound to the surface *via* oxygen atoms is reasonable in view of the reactive groups on the quartz surface. Such a chemical reaction with the surface should be favoured at higher temperatures due to the likely energy barrier of the reaction. If the polonium would be irreversibly bound to the surface, a typical deposition peak of mobile adsorption would not be expected in the thermochromatogram due to the exponential temperature dependence of the reaction. Instead, a rather sharp increase and then a roughly exponential decline in the deposition would result with decreasing temperature. Since this exponential pattern is not observed, it is plausible that the polonium species formed on the surface was again desorbed from the surface after the reaction and transported further through the column to the final deposition zone. On the basis of the previous experiments, a lower deposition temperature would be expected for the deposition of elemental polonium. Thus, it is plausible that an oxidized polonium compound formed *via* the reaction with the quartz surface was deposited at (277 ± 5) °C. However, the employed thermochromatography method does not allow a direct speciation of the formed polonium species. Further speciation with classical spectroscopy or microscopy techniques was also not possible due to the single-atom nature of the experiments. Accordingly, we cannot infer a reaction mechanism from our measurements. The adsorption enthalpy of the low-temperature species coincides with the adsorption enthalpy assigned to elemental polonium in experiments **He$_{Q1}$**, **He$_{Q2}$** and **He$_{Q1}$ II**. Consequently, the minor deposition at (67 ± 5) °C is assigned to elemental polonium. This may indicate that some of the polonium has not reacted with the quartz surface.

To study the influence of a reducing environment on the polonium deposition, a mixture of 10% hydrogen and 90% helium was used in experiment **H2$_{Q3}$**. The quartz surface remained untreated (Q3) as in experiment **He$_{Q3}$** (Fig. 4). The resulting distribution of activity is shown in Fig. 6. Two depositions peaks were detected at T_{dep} = (320 ± 10) °C ((48 ± 2)% of the total activity) and T_{dep} = (70 ± 7) °C ((37 ± 2)% of the total activity). The remaining activity was deposited at the very beginning of the chromatography column as a tail starting at

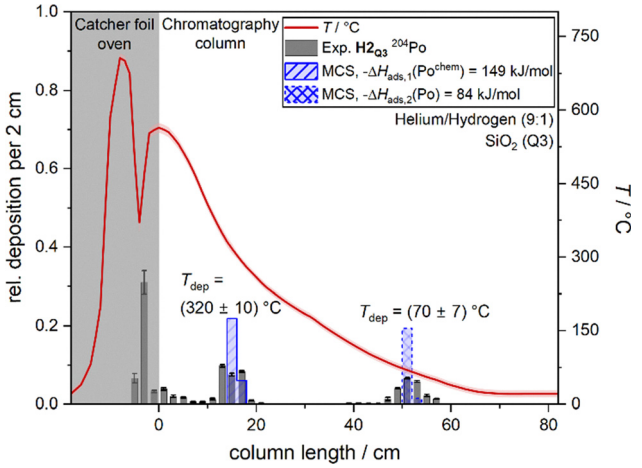

Fig. 6 Thermochromatogram of ^{204}Po under helium/hydrogen atmospheres on quartz glass Q3. The experimental depositions are shown in grey, the simulated deposition using the Monte Carlo simulation (MCS) is shown in blue and the temperature gradient is shown in red. The relative area of the simulated deposition was scaled to the relative area of the experimental peaks. Here, $-\Delta H_{ads}$ is the adsorption enthalpy and T_{dep} is the deposition temperature at the peak maximum. Depositions upstream of the chromatography column and downstream of the oven to bake-out the catcher foil are shown on a gray background.

the highest temperature of (560 ± 10) °C. The deposition upstream of the column part relevant for chromatography and downstream of the oven for baking-out the catcher foil is also shown. A significant deposition was measured in the transport line from the catcher foil oven to the column part relevant for chromatography. In this section, the minimum temperature of (360 ± 20) °C is similar to the deposition temperature of T_{dep} = (320 ± 10) °C in the column. Thus, both depositions are assigned to the same species. Using the Monte Carlo simulation, the adsorption enthalpy of $-\Delta H_{ads}(Po^{chem}) = 149^{+4}_{-6}$ kJ mol^{-1} was obtained from the deposition temperature for the high-temperature deposition and the adsorption enthalpy of $-\Delta H_{ads}(Po) = 84^{+4}_{-5}$ kJ mol^{-1} for the deposition at (70 ± 7) °C in experiment **H2$_{Q3}$**. The adsorption enthalpy of the high-temperature deposition agrees within the error bar with that of the main deposition peak in experiment **He$_{Q3}$**. The adsorption enthalpy of the low-temperature species corresponds to the adsorption enthalpies obtained in experiments **He$_{Q1}$**, **He$_{Q2}$** and **He$_{Q1}$ II**, which were assigned to elemental polonium. Thus, elemental polonium was deposited at (70 ± 7) °C in this experiment. This supports the assignment of previous low-temperature depositions to elemental polonium, as oxidized species formed in the gas phase are unlikely to be present in this experiment due to the reducing atmosphere. Since two species were observed in the experiment **H2$_{Q3}$**, the assumption quickly arises that polonium could have reacted with the added hydrogen to form H_2Po. However, as already discussed in the introduction, polonium hydride would be expected to be more volatile than elemental polonium.[1,22] Thus, the higher absolute value of the adsorption enthalpy of $-\Delta H_{ads}(Po^{chem}) = 149^{+4}_{-6}$ kJ mol^{-1} does not match the properties of the hydride. Adding to this, the hydride would not be stable under the selected conditions (high temperatures and exposure to light).[1] Therefore, the presence of polonium hydride in the column is excluded. This is in agreement with interpretations of previous thermochromatographic studies of polonium under a hydrogen atmosphere.[46,48,49] As the same quartz glass was used in experiment **H2$_{Q3}$** as in experiment **He$_{Q3}$**, it is most likely that a chemical reaction of polonium with the quartz surface was the cause for this deposition also in experiment **H2$_{Q3}$**. This is further sustained by the known fact that hydrogen can react with siloxane groups on the quartz surface. Although the exact reaction mechanism is debated, silanol groups are formed in all suggested reaction pathways.[35,36] Such a modification of the quartz surface due to a reaction with hydrogen during the experiment would make the surface even more reactive and a reaction of polonium with the silanol groups would be even more favoured. As discussed above, desorption of polonium as an oxidized species after the reaction with the surface seems likely. It is possible that the desorbed oxygen-containing species is subsequently reduced again to elemental polonium by hydrogen in the gas phase. This would explain that the fraction of polonium deposited at (70 ± 7) °C is larger in experiment **H2$_{Q3}$** than in experiment **He$_{Q3}$**.

Various studies of the reactivity of polonium on quartz have already been carried out. The adsorption enthalpy values of elemental polonium determined in ref. 46–48 all agree with the adsorption enthalpy determined for elemental polonium in this work. Isothermal chromatography was used in these literature works in contrast to thermochromatography used in the present work. In isothermal chromatography, the temperature of the column is changed with each measurement. With this method, reactions with the surface at lower column temperatures (below 300 °C) are less likely, as polonium does not come into contact with a hot (and therefore more reactive) quartz surface immediately after entering the column. In thermochromatography where a negative temperature gradient is applied, the hottest area is located directly at the beginning of the column, which makes reactions with the quartz surface more probable. The adsorption enthalpy values published in ref. 49 and 57 agree with or are similar to the adsorption enthalpies determined for the deposition of polonium on more reactive quartz surfaces as used in this work. As in our study, thermochromatography was used in ref. 49. Thus, we were able to confirm the adsorption enthalpies of polonium on quartz determined in several past experiments. Our data indicate that the differences in the published enthalpies are due to differences in the reactivity of the employed quartz types.

Conclusions

Thermochromatography experiments in pure helium allowed the adsorption enthalpy of elemental polonium on weakly reactive quartz surfaces (Q1 and Q2, respectively) to be determined as $-\Delta H_{ads}(Po) = 85^{+3}_{-2}$ kJ mol^{-1}, which agrees with the literature.[46–48] On a more hydroxylated quartz surface (Q3), a higher absolute value of the adsorption enthalpy of $-\Delta H_{ads}(Po^{chem}) = 139^{+6}_{-5}$ kJ mol^{-1} was obtained and attributed to a different species formed by the chemical reaction of polonium with the quartz surface. This species is most likely

an oxygen-containing species. It was found that polonium does not react with hydrogen in the gas phase which is in agreement with previous experiments.[46,48,49]

Consequently, we show that a surface reaction can be as decisive for the observed deposition pattern as reactions in the gas phase in gas chromatography experiments with homologues of superheavy elements and thus potentially also with SHE. In the future, more attention should therefore be paid to the exact structure of the surface. The thermal history and type of production should always be known, especially in the case of quartz. In addition, analytical methods should be established with which the density of silanol groups on the surface can be determined.

Author contributions

Katharina Hermainski: conceptualization, formal analysis, investigation, and writing – original draft; Alexander Yakushev: conceptualization, investigation, methodology, supervision, validation, and writing – review and editing; Dominik Dietzel: conceptualization, investigation, and writing – review and editing; Christoph Emanuel Düllmann: funding acquisition, investigation, supervision, validation, and writing – review and editing; Jochen Ballof, Pavol Mošat' and Felix Sprunk: investigation and writing – review and editing; Pavel Bartl, Jan John, Mojmír Němec, Jon Petter Omtvedt and Jan Štursa: investigation, resources, and writing – review and editing; Jörg Krier: resources and writing – review editing.

Conflicts of interest

There are no conflicts to declare.

Data availability

Data supporting this article have been included as part of the SI. See DOI: **https://doi.org/10.1039/d5cp02381e**.

The raw data are available from the corresponding author upon reasonable request.

Acknowledgements

The authors thank R. Jera and B. Schrohe for preparing the quartz glass columns of type Q2. They also thank the cyclotron operators at the Nuclear Physics Institute in Řež for providing a stable beam for our experiments, and R. A. Cantemir for printing the sample holder. The experiments were performed in the frame of FAIR Phase-0. This work was funded by the Federal Ministry of Education and Research of Germany (project number 05P21UMFN2) and the Facility for Antiproton and Ion Research – Participation of the Czech Republic (FAIR-CZ), Project Number LM2023060, supported by the Ministry of Education, Youth and Sports of the Czech Republic.

Notes and references

1 K. W. Bagnall, in *Comprehensive inorganic chemistry*, ed. J. C. Bailar, H. J. Emeléus, Sir R. Nyholm and A. F. Trotman-Dickenson, Pergamon Press, Oxford, 1st edn, 1973, ch. 23-24, pp. 935–1008.
2 P. Thakur and A. L. Ward, *J. Radioanal. Nucl. Chem.*, 2020, **323**, 27–49.
3 B. R. R. Persson and E. Holm, *J. Environ. Radioact.*, 2011, **102**, 420–429.
4 C. D. Bowman, *Annu. Rev. Nucl. Part. Sci.*, 1998, **48**, 505–556.
5 E. A. Maugeri, J. Neuhausen, R. Eichler, R. Dressler, K. Rijpstra, S. Cottenier, D. Piguet, A. Vögele and D. Schumann, *Radiochim. Acta*, 2016, **104**, 757–767.
6 E. A. Maugeri, J. Neuhausen, R. Eichler, R. Dressler, K. Rijpstra, S. Cottenier, D. Piguet, A. Vögele and D. Schumann, *Radiochim. Acta*, 2016, **104**, 769–779.
7 E. A. Maugeri, J. Neuhausen, B. G. Prieto, A. Aerts, T. M. Mendonça, T. Stora and R. Eichler, *Radiochim. Acta*, 2018, **106**, 125–134.
8 I. Zvára, Y. U. Chuburkov, R. Caletka, T. S. Zvarova, M. P. Shalaevskii and B. V. Shilov, *J. Nucl. Energy*, 1967, **21**, 601–603.
9 R. Silva, J. Harris, M. Nurmia, K. Eskola and A. Ghiorso, *Inorg. Nucl. Chem. Lett.*, 1970, **6**, 871–877.
10 A. Türler and V. Pershina, *Chem. Rev.*, 2013, **113**, 1237–1312.
11 M. Schädel and D. Shaughnessy, *The Chemistry of Superheavy Elements*, Springer, Berlin, 2014.
12 A. Yakushev, J. Khuyagbaatar, Ch. E. Düllmann, M. Block, R. A. Cantemir, D. M. Cox, D. Dietzel, F. Giacoppo, Y. Hrabar, M. Iliaš, E. Jäger, J. Krier, D. Krupp, N. Kurz, L. Lens, S. Löchner, C. Mokry, P. Mošať, V. Pershina, S. Raeder, D. Rudolph, J. Runke, L. G. Sarmiento, B. Schausten, U. Scherer, P. Thörle-Pospiech, N. Trautmann, M. Wegrzecki and P. Wieczorek, *Front. Chem.*, 2024, **12**, 1474820.
13 P. Schwerdtfeger, O. R. Smits and P. Pyykkö, *Nat. Rev. Chem.*, 2020, **4**, 359–380.
14 Y. T. Oganessian and V. K. Utyonkov, *Rep. Prog. Phys.*, 2015, **78**, 36301.
15 S. A. Giuliani, Z. Matheson, W. Nazarewicz, E. Olsen, P.-G. Reinhard, J. Sadhukhan, B. Schuetrumpf, N. Schunck and P. Schwerdtfeger, *Rev. Mod. Phys.*, 2019, **91**, 11001.
16 C. Morse, *Nucl. Data Sheets*, 2022, **182**, 167–202.
17 H. Wiberg, *Lehrbuch der Anorganischen Chemie*, Walter de Gruyter, Berlin, 2007.
18 N. N. Greenwood and A. Earnshaw, *Chemistry of the elements*, Elsevier, Amsterdam, 2nd edn, 1997, ch. 16, 747–788.
19 K. W. Bagnall and R. W. M. D'Eye, *J. Chem. Soc.*, 1954, **1**, 4295–4299.
20 A. S. Abakumov, *Russ. Chem. Rev.*, 1982, **51**, 1091–1102.
21 K. W. Bagnall, *Radiochim. Acta*, 1983, **32**, 153–161.
22 F. Weigel, *Angew. Chem., Int. Ed. Engl.*, 1959, **71**, 289–316.
23 A. F. Novgorodov, F. Rösch and N. A. Korolev, *Handbook of Nuclear Chemistry - Instrumentation, separation techniques, environmental issues*, ed A. Vertés, S. Nagy, Z. Klencsár,

R. G. Lovas and F. Rösch, Springer, Dordrecht, 2nd edn, 2011, ch. 53, 2429–2458.
24 S. Soverna, R. Dressler, Ch. E. Düllmann, B. Eichler, R. Eichler, H. W. Gäggeler, F. Haenssler, J.-P. Niklaus, D. Piguet, Z. Qin, A. Türler and A. B. Yakushev, *Radiochim. Acta*, 2005, **93**, 1–8.
25 A. H. W. Aten, *Adv. Inorg. Chem. Radiochem.*, 1964, **6**, 207–223.
26 N. C. Norman, *Chemistry of arsenic, antimony and bismuth*, Blackie Academic & Professional, London, 1998.
27 J. S. Casas and J. Sordo, *Lead - Chemistry, analytical aspects, environmental impact and health effects*, Elsevier, Oxford, 2006.
28 G.-J. Meyer, *J. Label. Compd. Radiopharm.*, 2018, **61**, 154–164.
29 A. Serov, R. Eichler, R. Dressler, D. Piguet, A. Türler, A. Vögele, D. Wittwer and H. W. Gäggeler, *Radiochim. Acta*, 2013, **101**, 421–426.
30 V. Pershina, *Radiochim. Acta*, 2011, **99**, 459–476.
31 R. H. Doremus, *Annu. Rev. Mater. Sci.*, 1972, **2**, 93–120.
32 G. A. Parks, *J. Geophys. Res.*, 1984, **89**, 3997–4008.
33 I. Zvára, *The inorganic radiochemistry of heavy elements*, Springer, Luxembourg, 2008.
34 H.-P. Boehm, *Angew. Chem., Int. Ed. Engl.*, 1966, **5**, 533–622.
35 J. E. Shelby, *J. Non-Cryst. Solids*, 1994, **179**, 138–147.
36 A. P. Velmuzhov, M. V. Sukhanov, M. F. Churbanov, T. V. Kotereva, L. V. Shabarova and Y. P. Kirillov, *Inorg. Mater.*, 2018, **54**, 925–930.
37 J. E. Shelby, *J. Appl. Phys.*, 1980, **51**, 2589–2593.
38 J. Stone, *J. Light Technol.*, 1987, **5**, 712–733.
39 P. B. McGinnis and J. E. Shelby, *J. Non-Cryst. Solids*, 1994, **179**, 185–193.
40 B. C. Schmidt, F. M. Holtz and J.-M. Bény, *J. Non-Cryst. Solids*, 1998, **240**, 91–103.
41 P. Atkins and J. de Paula, *Atkins' physical chemistry*, Oxford University Press, Oxford, 2006.
42 A. Yakushev, L. Lens, Ch. E. Düllmann, J. Khuyagbaatar, E. Jäger, J. Krier, J. Runke, H. M. Albers, M. Asai, M. Block, J. Despotopulos, A. Di Nitto, K. Eberhardt, U. Forsberg, P. Golubev, M. Götz, S. Götz, H. Haba, L. Harkness-Brennan, R.-D. Herzberg, F. P. Heßberger, D. Hinde, A. Hübner, D. Judson, B. Kindler, Y. Komori, J. Konki, J. V. Kratz, N. Kurz, M. Laatiaoui, S. Lahiri, B. Lommel, M. Maiti, A. K. Mistry, C. Mokry, K. J. Moody, Y. Nagame, J. P. Omtvedt, P. Papadakis, V. Pershina, D. Rudolph, L. G. Samiento, T. K. Sato, M. Schädel, P. Scharrer, B. Schausten, D. A. Shaughnessy, J. Steiner, P. Thörle-Pospiech, A. Toyoshima, N. Trautmann, K. Tsukada, J. Uusitalo, K.-O. Voss, A. Ward, M. Wegrzecki, N. Wiehl, E. Williams and V. Yakusheva, *Front. Chem.*, 2022, **10**, 976635.
43 I. Zvára, *Radiochim. Acta*, 1985, **38**, 95–101.
44 J. Even, A. Yakushev, Ch. E. Düllmann, H. Haba, M. Asai, T. K. Sato, H. Brand, A. Di Nitto, R. Eichler, F. L. Fan, W. Hartmann, M. Huang, E. Jäger, D. Kaji, J. Kanaya, Y. Kaneya, J. Khuyagbaatar, B. Kindler, J. V. Kratz, J. Krier, Y. Kudou, N. Kurz, B. Lommel, S. Miyashita, K. Morimoto, K. Morita, M. Murakami, Y. Nagame, H. Nitsche, K. Ooe, Z. Qin, M. Schädel, J. Steiner, T. Sumita, M. Takeyama, K. Tanaka, A. Toyoshima, K. Tsukada, A. Türler, I. Usoltsev, Y. Wakabayashi, Y. Wang, N. Wiehl and S. Yamaki, *Science*, 2014, **345**, 1491–1493.
45 R. Eichler, N. V. Aksenov, A. V. Belozerov, G. A. Bozhikov, V. I. Chepigin, S. N. Dmitriev, R. Dressler, H. W. Gäggeler, V. A. Gorshkov, F. Haenssler, M. G. Itkis, A. Laube, V. Y. Lebedev, O. N. Malyshev, Y. T. Oganessian, O. V. Petrushkin, D. Piguet, P. Rasmussen, S. V. Shishkin, A. V. Shutov, A. I. Svirikhin, E. E. Tereshatov, G. K. Vostokin, M. Wegrzecki and A. V. Yeremin, *Nature*, 2007, **447**, 72–75.
46 B. Eichler, *Kernenergie*, 1976, **19**, 307–311.
47 A. Vogt, H. W. Gäggeler and A. Türler, *Adsorption gas chromatography with 150-ms 216-Po*, Paul Scherrer Institut, Villingen, 1996.
48 M. Gärtner, PhD Thesis, University Bern, 2001.
49 E. A. Maugeri, J. Neuhausen, R. Eichler, D. Piguet, T. M. Mendonça, T. Stora and D. Schumann, *J. Nucl. Mater.*, 2014, **450**, 292–298.
50 P. Bartl, R. Běhal, T. Matlocha, M. Němec, P. Šváb, V. Zach, A. Bulíková, J. Štursa, J. P. Omtvedt and J. John, *Nucl. Instrum. Methods Phys. Res., Sect. A*, 2023, **1052**, 168280.
51 B. Eichler and R. Eichler, *The chemistry of superheavy elements*, ed M. Schädel and D. Shaughnessy, Springer, Berlin, 2nd edn, 2014, ch. 7, pp. 375–413.
52 E. A. Maugeri, J. Neuhausen, R. Eichler, D. Piguet and D. Schumann, *J. Nucl. Mater.*, 2014, **452**, 110–117.
53 H.-J. Freund, B. Dillmann, O. Seiferth, G. Klivenyi, M. Bender, D. Ehrlich, I. Hemmerich and D. Cappus, *Catal. Today*, 1996, **32**, 1–10.
54 J. A. Kelber, *Surf. Sci. Rep.*, 2007, **62**, 271–303.
55 M. Heemeier, M. Frank, J. Libuda, K. Wolter, H. Kuhlenbeck, M. Bäumer and H.-J. Freund, *Catal. Lett.*, 2000, **68**, 19–24.
56 S. A. Chambers, T. Droubay, D. R. Jennison and T. R. Mattsson, *Science*, 2002, **297**, 827–831.
57 H. Gäggeler, H. Dornhöfer, W. D. Schmidt-Ott, N. Greulich and B. Eichler, *Radiochim. Acta*, 1985, **38**, 103–106.

